24th INTERNATIONAL CONGRESS ON SOUND AND VIBRATION
23–27 July 2017, London

ICSV24
23-27JULY 2017
LONDON CALLING

APPLICATION OF ADDED MASS CONCEPT OF BENDING VIBRATION TO THE DESIGN OF A LEVEL-SWITCH SENSOR

Jin Oh Kim, Jeong Gil Hwang, Sang Ok Seon and Chunguang Piao

Soongsil University, Department of Mechanical Engineering, Seoul, Korea
email: jokim@ssu.ac.kr

This paper deals with the added mass of fluid around a cantilever rod vibrating transversely. This study is necessary to design a level switch sensor because its sensitivity depends on the change of the natural frequency in the presence of added mass effect. We considered solid and hollow cross-sections of elliptic and rectangular shapes with various aspect ratios and thicknesses. Stream function and velocity potential were obtained theoretically and numerically in the fluid adjacent to the rod, and the results yielded the added mass effect on the natural frequency of the bending vibration of the rod. After verifying numerical scheme by comparing its result with analytical one for a circular cross-section, we calculated numerically the effect of the added mass of fluid on the change of the natural frequency of a cantilever rod with various cross-sectional shapes. Experiments of modal testing support the calculated results. We showed the proportional relation of the sensor's sensitivity with the added mass effect and thus with the aspect ratio and thinness of the cross-section. The results of this study can be used to design the cross-sectional shape of the sensor to increase or decrease the sensitivity.
Keywords: bending vibration, stream function, added mass, natural frequency, level switch

1. Introduction

A level-switch sensor using bending vibration is one of the devices measuring liquid or powder height [1]. It detects the presence of a medium at a particular height, based on the difference of the characteristics of bending vibration of a rod in air and in the medium [2,3]. The natural frequency and amplitude of the vibration of a rod decrease in liquid because of the added mass effect, which depends on the cross-sectional shape of the rod. Therefore, it is necessary to identify the added mass effect according to the shape of the cross-section in order to design the cross-sectional shape of the sensor rod increasing or decreasing the sensitivity.

Kongthon et al. [4] presented the added-mass effect of cilia-based devices for microfluidic systems by modeling them as a rectangular cantilever. They reported the reduction of the natural frequency in the presence of the added mass. Sedlar et al. [5] experimentally investigated the added mass of the cantilever beam partially submerged in water. Zheng et al. [6] presented the design and theoretical analysis of a resonant sensor for liquid density measurement. They considered a tuning fork type sensor and reported the reduction of the natural frequency according to the mass density of liquid. Yeh [7] presented a theoretical method of calculating the natural frequencies of a free-free beam under liquids of various densities. He investigated the mechanism causing the change of frequency in water. Blake [8] theoretically and experimentally investigated the acoustic radiation from free-free beams vibrating transversely. Konstantinidis [9] dealt with added mass of a circular cylinder oscillating in a free stream. Zhu et al. [10] derived the added mass coefficient and the water level index formulas for bulkheads of rectangular liquid tanks.

Based on the well-known theory on the transverse vibration of a cantilever rod [11], this paper deals with added mass of solid and hollow cross-sections of elliptic and rectangular shapes with

various aspect ratios and thicknesses. For some particular shapes, such as circular and elliptic shapes, the added mass is expressed theoretically from stream function or velocity potential [12]. After verifying a numerical scheme by comparing their results with the theoretically obtained results [13], the scheme is used to solid and hollow rectangular shapes of various aspect ratios and thicknesses. Modal testing experimentally supports the numerical results by comparing the natural frequency change related with the added mass effect. The sensor's sensitivity is related with the added mass and thus with the aspect ratio and the thickness of the cross-section.

2. Theoretical analysis

A cantilever rod in liquid is schematically shown in Fig. 1. Transverse motion of the rod is affected by the added mass, or virtual mass in other words, of adjacent liquid. In this section, the added mass is obtained theoretically and it is related with the sensor's sensitivity.

The bending vibration of a cantilever rod can be described by the Euler-Bernoulli beam theory [11]. In the absence of liquid, the equation of motion of the bending vibration is expressed in terms of the transverse displacement $w(x,t)$ as follows:

$$\frac{\partial^2 w(x,t)}{\partial t^2} + c^2 \frac{\partial^2 w(x,t)}{\partial x^2} = 0, \qquad c = \sqrt{\frac{E\,I}{\rho_s\,A_s}} \tag{1}$$

where ρ_s, E, A_s and I are the mass density, Young's modulus, cross-sectional area, area moment of inertia of the cross-section, respectively. The transverse displacement can be expressed as $w(x,t) = W(x)\,\exp(i\omega t)$ by separation of variables for the rod vibrating with frequency ω. Then, Eq. (1) is rewritten as follows:

$$\frac{d^4 W}{dx^4} - \beta^4 W = 0, \qquad \beta = \sqrt{\frac{\omega}{c}} \tag{2}$$

Boundary conditions of a cantilever rod are

$$W(0) = 0 \quad \text{and} \quad W'(0) = 0 \quad \text{at} \quad x = 0 \tag{3a,b}$$

$$W''(L) = 0 \quad \text{and} \quad W'''(L) = 0 \quad \text{at} \quad x = L \tag{3c,d}$$

The characteristic equation satisfying Eq. (3) is as follows [11]:

$$\beta^6 \left[\cos(\beta L)\,\cosh(\beta L) + 1\right] = 0 \tag{4}$$

Non-trivial roots of Eq. (4) are βL = 1.875, 4.694, 7.855, … The frequency in Hz unit is

$$f_0 = \frac{(\beta L)^2}{2\pi}\sqrt{\frac{E\,I}{\rho_s\,A_s\,L^4}} \tag{5}$$

Eq. (5) expresses the natural frequency of a cantilever rod in air.

When the cantilever rod is fully submerged in liquid, its natural frequency is affected by the added mass of liquid as follows [14]:

$$f = \frac{(\beta L)^2}{2\pi}\sqrt{\frac{E\,I}{\left(\rho_s A_s + \rho_f A_f\right)L^4}} \tag{6}$$

where ρ_f and A_f are the mass density and added area of liquid, respectively. Here, $\rho_f\,A_f$ means the added mass per unit length of the rod. The added area and the added mass are dependent on the cross-sectional shape of the rod.

The irrotational motion of ideal liquid can be expressed in terms of stream function ψ and velocity potential ϕ as follows [12]:

$$\nabla^2 \psi = 0 \quad \text{and} \quad \nabla^2 \phi = 0 \tag{7a,b}$$

Kinetic energy per unit length of liquid is [12]

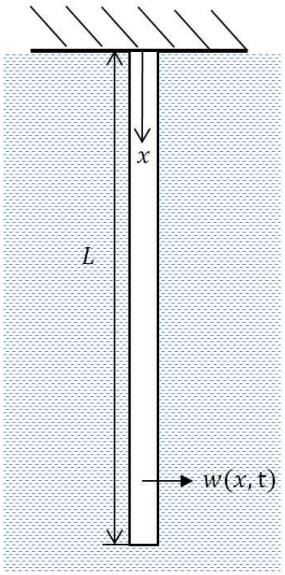

Figure 1: Schematic diagram of a cantilever rod in liquid.

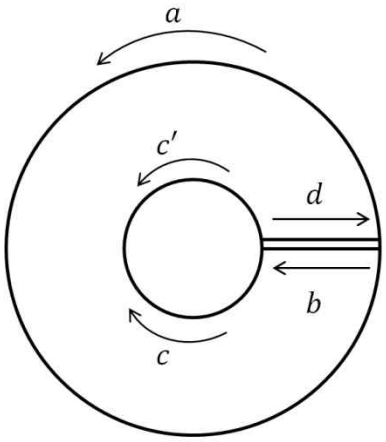

Figure 2: Lines of the contour integral.

$$T = \frac{1}{2}\rho_f \iint \nabla\psi \cdot \nabla\psi \, dA = -\frac{1}{2}\rho_f \oint \psi \frac{\partial \psi}{\partial n} \, ds \tag{8a}$$

$$T = \frac{1}{2}\rho_f \iint \nabla\phi \cdot \nabla\phi \, dA = -\frac{1}{2}\rho_f \oint \phi \frac{\partial \phi}{\partial n} \, ds \tag{8b}$$

The contour integral in Eq. (8) can be conducted along the lines shown in Fig. 2. The integral along line (a) is zero because the velocity potential or stream function in negligibly small. The integrals along lines (b) and (d) cancel each other. Therefore, Eq. (8) becomes line integral along the contour of the rod cross-section as follows:

$$T = \frac{1}{2}\rho_f \int_c \psi \frac{\partial \psi}{\partial n} \, ds = \frac{1}{2}\rho_f \int_c \phi \frac{\partial \phi}{\partial n} \, ds \tag{9}$$

When the rod oscillates transversely with the velocity amplitude $U(x)$ in liquid, the maximum kinetic energy per unit length is $T = \frac{1}{2}\rho_f \, A_f \, U^2$, and the added area is

$$A_f = \frac{1}{U^2} \int_c \psi \frac{\partial \psi}{\partial n} \, ds = \frac{1}{U^2} \int_c \phi \frac{\partial \phi}{\partial n} \, ds \tag{10}$$

Examples of the cross-sectional shapes of a rod are shown in Fig. 3.

For a circular cross-section of a rod moving transversely with velocity U in a stationary liquid, the velocity of liquid at the boundary of the rod is

$$V_r \left(= -\frac{1}{r}\frac{\partial \psi}{\partial \theta} = -\frac{\partial \phi}{\partial r} \right) = U \cos\theta \qquad \text{at} \quad r = a \tag{11}$$

The solution of Eq. (7) satisfying the boundary condition (11) is [12]

$$\psi = -\frac{U a^2}{r} \sin\theta, \qquad \phi = \frac{U a^2}{r} \cos\theta \tag{12a,b}$$

The velocity potential curves are displayed in Fig. 4(a) from the velocity potential function ϕ of Eq. (12b). Line integral of Eq. (10) with Eq. (12) yields

$$A_f = a^2 \int_0^{2\pi} \cos^2\theta \, d\theta = \pi \, a^2 \tag{13}$$

Therefore, A_f / A_s is 1 for a circular shape.

For an elliptic cross-section of a rod moving transversely with velocity U as shown in Fig. 3(a), elliptic coordinates ξ and η are introduced for the analysis as follows [12]:

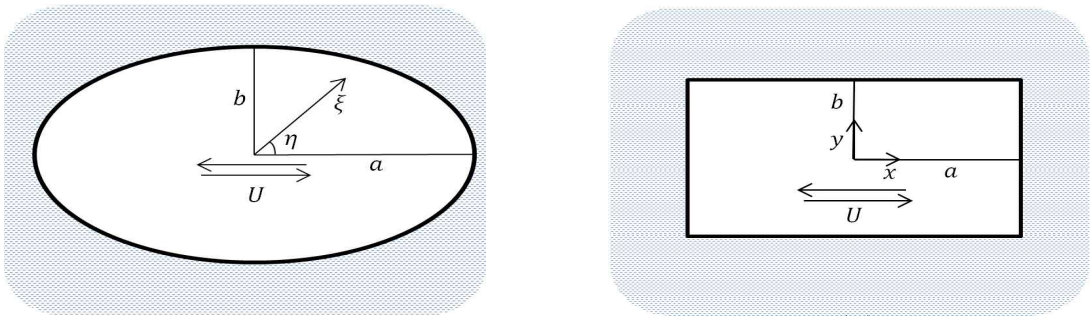

(a) (b)

Figure 3: Cross-section of a cantilever rod; (a) ellipse, (b) rectangle.

$$x = c \cosh\xi \cos\eta, \quad y = c \sinh\xi \sin\eta \tag{14a,b}$$

The solution of Eq. (7) is

$$\psi = -U\, b \left(\frac{a+b}{a-b}\right)^{1/2} e^{-\xi} \sin\eta, \quad \phi = U\, b \left(\frac{a+b}{a-b}\right)^{1/2} e^{-\xi} \cos\eta \tag{15}$$

Line integral of Eq. (10) with Eq. (15) yields

$$A_f = b^2 \int_0^{2\pi} \cos^2\eta \, d\eta = \pi\, b^2 \tag{16}$$

Therefore A_f / A_s is b/a for an elliptic shape.

For a rectangular cross-section, the velocity potential and added mass are calculated numerically in Section 3.

The frequency f expressed in Eq. (6) can be rearranged as follows:

$$\begin{aligned} f &= f_0 \left(1 + \frac{\rho_f\, A_f}{\rho_s\, A_s}\right)^{-1/2} \\ &= f_0 \left[1 - \frac{1}{2}\frac{\rho_f\, A_f}{\rho_s\, A_s} + \frac{3}{8}\left(\frac{\rho_f\, A_f}{\rho_s\, A_s}\right)^2 - \frac{5}{16}\left(\frac{\rho_f\, A_f}{\rho_s\, A_s}\right)^3 + \cdots\right] \end{aligned} \tag{17}$$

The difference Δf of the frequencies f and f_0 is normalized by f_0 as follows:

$$\frac{\Delta f}{f_0} = -\frac{1}{2}\frac{\rho_f\, A_f}{\rho_s\, A_s} + \frac{3}{8}\left(\frac{\rho_f\, A_f}{\rho_s\, A_s}\right)^2 - \frac{5}{16}\left(\frac{\rho_f\, A_f}{\rho_s\, A_s}\right)^3 + \cdots \tag{18}$$

When $(\rho_f\, A_f)/(\rho_s\, A_s)$ is much smaller than 1, Eq. (18) can be approximated as follows:

$$\frac{\Delta f}{f_0} \approx -\frac{1}{2}\frac{\rho_f\, A_f}{\rho_s\, A_s} \propto -\frac{A_f}{A_s} \tag{19}$$

It means that the frequency difference Δf normalized by the natural frequency in air f_0 is linearly proportional to the area ratio A_f / A_s. The sensitivity of the level-switch sensor depends on $\Delta f / f_0$ and thus on A_f / A_s.

3. Comparison with FEA and experiment

The added mass for arbitrary shape of the cross-section can be obtained by the finite element analysis. The theoretical results are compared with experiments for verification.

For an arbitrary cross-section, such as a square and a rectangle, the added area can be obtained numerically by the finite element analysis. We used a commercial software ANSYS. Mathematically, potential flow problem has similarity with steady-state heat conduction problem. The governing equation is Laplace equation as follows [15]:

$$\nabla^2 T = 0 \tag{23}$$

where T is temperature. Boundary condition for flow velocity $\partial\phi/\partial n$ corresponds to heat flux $\partial T/\partial n$.

Before calculating the added area for an arbitrary cross-section, the finite element analysis was carried out and compared with the theoretical result for a circular cross-section. The boundary condition (11) corresponds to the following expression:

$$\frac{\partial T}{\partial r} = -U\cos\theta \qquad \text{at} \qquad r = a \tag{24}$$

The velocity potential around a circular cross-section was calculated and displayed in Fig. 4(b). The result is quite similar to the theoretical one shown in Fig. 4(a). The added area is calculated numerically from the stream function or the velocity potential function as follows:

$$A_f = \frac{1}{U^2}\sum \psi \frac{\Delta\psi}{\Delta n}\Delta s = \frac{1}{U^2}\sum \phi \frac{\Delta\phi}{\Delta n}\Delta s \tag{25}$$

The ratio of added area A_f and cross-sectional area A_s for circular cross-section was 0.984. The numerically obtained value is accurate within 1.6% error.

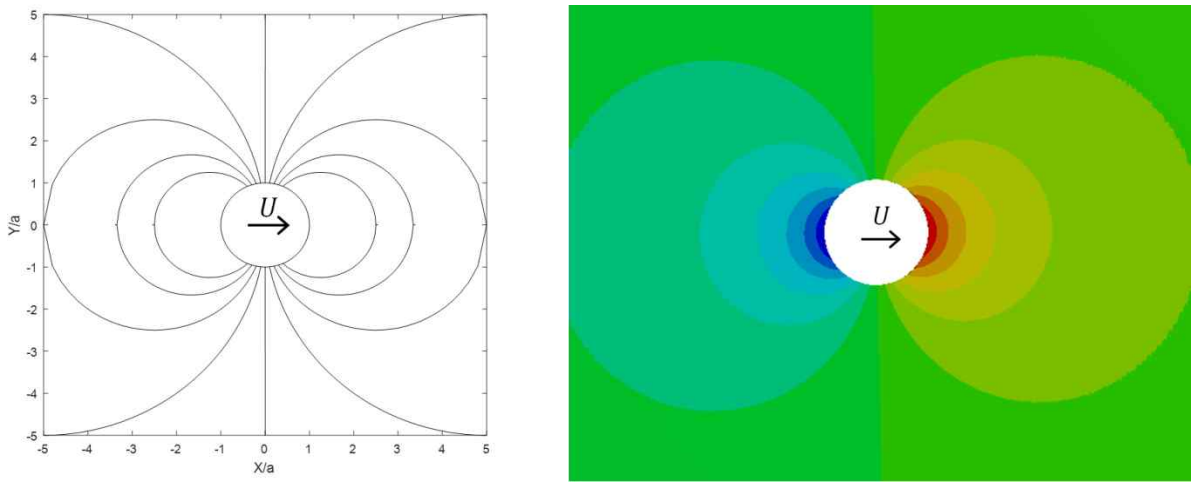

(a) (b)

Figure 4: Velocity potential curves around a circle; (a) theoretical analysis, (b) finite element analysis.

For a square or a rectangle, flow velocity is U along the lines normal to the motion and zero along the lines parallel to the motion. The results are displayed in Fig. 5 as velocity potential curves. The numerical values of A_f/A_s ratio for rectangular cross-section are calculated for aspect ratio $b/a = 0.5$, 1 and 2.

In order to compare the theoretical results with experimental ones, the first natural frequency was measured by modal testing method. The experimental equipment consists of vibration sensors, a conditioning amplifier, and a signal analyzer, as schematically shown in Fig. 6. The measured FRF (frequency response function) curves reveal natural frequencies at the peaks.

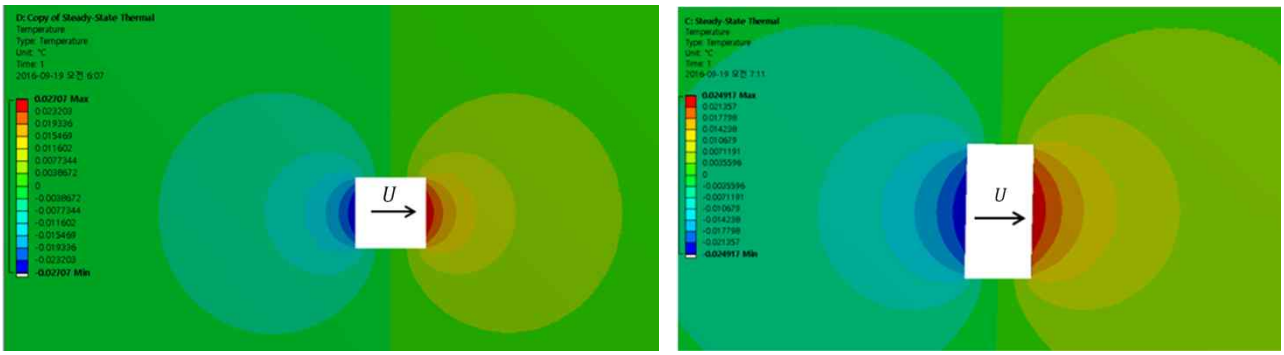

(a) (b)

Figure 5: Velocity potential curves obtained by the finite element analysis; (a) square, (b) rectangle.

The fundamental frequencies of the bending vibration of a rod in air are obtained for various cross-sections. The experimental results are compared with analytical results. The fundamental frequencies of a rod in water were calculated using Eq. (6) with the values of A_f / A_s.

The frequency reduction Δf is normalized by the frequency f_0. Theoretical (or finite element) analysis results and experimental results were calculated from the data. The approximate results were calculated from Eq. (19).

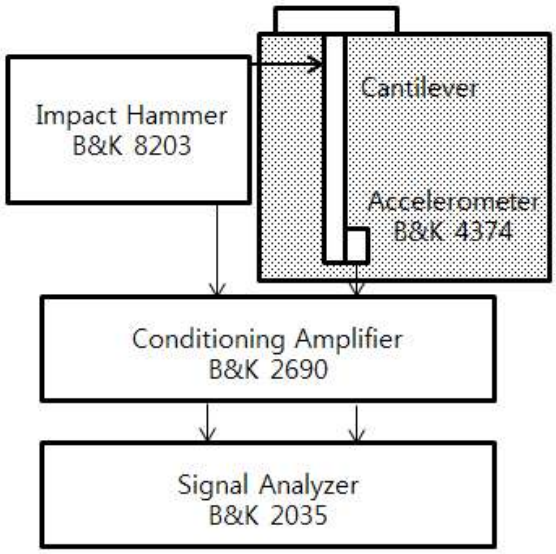

Figure 6: Experimental equipment.

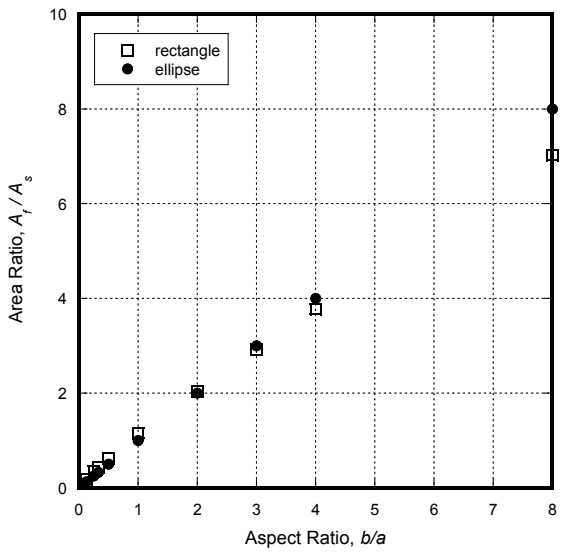

Figure 7: Area ratio A_f / A_s according to the aspect ratio b / a.

4. Design of a level-switch sensor

For the elliptic cross-section of a rod, the area ratio A_f / A_s $(= b / a)$ according to the aspect ratio b / a is displayed Fig. 7. For the rectangular cross-section of a rod, the area ratio is calculated by the finite-element analysis and the result is displayed in Fig. 7. The two results show similar trend.

For the elliptic hollow cross-section of a rod, the area ratio is displayed as a function of the thickness of the cross-section in Fig. 8(a). This figure shows the results for the aspect ratio b / a of 0.5, 1.0, and 2.0. The aspect ratio 1.0 corresponds to a circle.

For the rectangular cross-section of a rod, the area ratio is displayed as a function of the thickness of the cross-section in Fig. 8(b). This figure shows the results for the aspect ratio b / a of 0.5, 1.0, and 2.0. The aspect ratio 1.0 corresponds to a square.

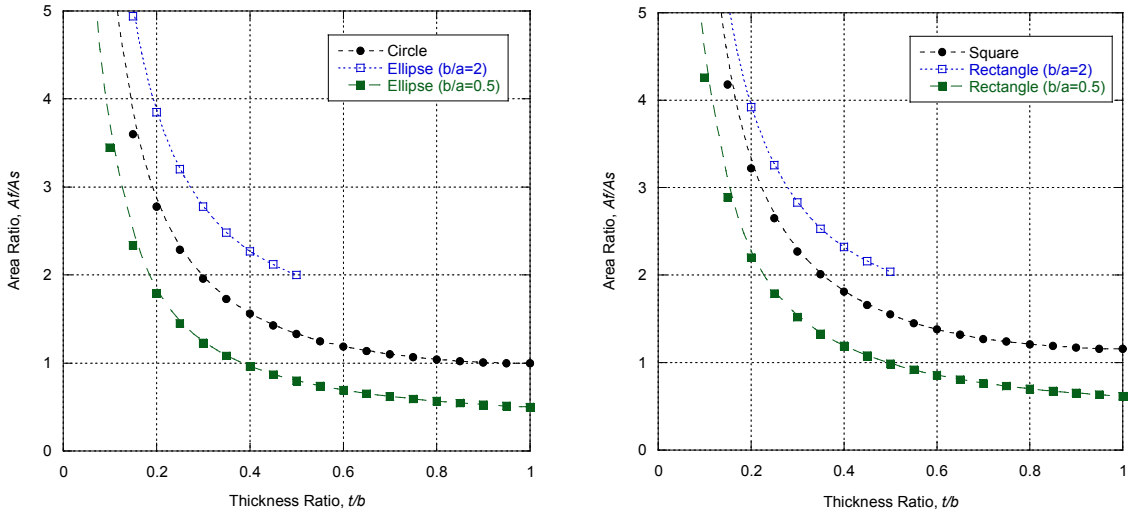

(a) (b)

Figure 8: Area ratio A_f / A_s according to the thickness ratio t / a for various aspect ratios; (a) hollow ellipse, (b) hollow rectangle.

5. Conclusion

This paper applied the added mass of liquid around a cantilever rod vibrating transversely to the design of a level-switch sensor. Stream function and velocity potential were obtained theoretically and numerically in the liquid adjacent to the rod, and the results yielded the added mass effect on the natural frequency of the bending vibration of the rod. After verifying numerical scheme by comparing its result with analytical one for a circular cross-section, we calculated numerically the effect of the added mass of liquid on the change of the natural frequency of a cantilever rod with solid and hollow cross-sections of rectangular shape. Experiments of modal testing support the calculated results.

We showed the relation of the sensor's sensitivity with the added mass and thus with the aspect ratio and thickness of the cross-section. The results of this study can be used to design the cross-sectional shape of the sensor rod increasing or decreasing the sensitivity depending on the change of the natural frequency in the presence of added mass effect.

REFERENCES

1 Lynnworth, L. C., *Ultrasonic Measurements for Process Control*, Academic Press, Boston, pp. 487-507 (1989).

2 Kim, J. O., Piao, C., Lee, S. H., Piezoelectric Transducer for Multiple Vibration Modes and Level Switch Sensor Comprising the Same, Korea Patent Application 10-2016-0143216 (2016).

3 Kim, J. O., Piao, C., Lee, S. H., Level Switch Sensor for Measuring Powder Level, Korea Patent Application 10-2016-0168413 (2016).

4 Kongthon, J., McKay, B., Iamratanakul, D., Oh, K., Chung, J.-H., Riley, J., Devasia, S., Added-Mass Effect in Modeling of Cilia-Based Devices for Microfluidic Systems, *Journal of Vibration and Acoustics*, **132**, 024501 (2010).

5 Sedlar, D., Lozina, Z., Vucina, D., Experimental Investigation of the Added Mass of the Cantilever Beam Partially Submerged in Water, *Technical Gazette*, **18** (4), 589-594 (2011).

6 Zheng, D., Shi, J., Fan, S., Design and Theoretical Analysis of a Resonant Sensor for Liquid Density Measurement, *Sensors*, **12**, 7905-7916 (2012).

7 Yeh, L., A Study of Vibration of Free-Free Beams under Liquid, *Annals of Nuclear Science and Engineering*, **1**, 437-450 (1974).

8 Blake, W. K., The Radiation from Free-Free Beams in Air and in Water, *Journal of Sound and Vibration*, **33** (4), 427-450 (1974).

9 Konstantinidis, E., Added Mass of a Circular Cylinder Oscillating in a Free Stream, *Proceedings of the Royal Society A*, **469**, 20130135 (2013).

10 Zhu, J., Lin, Z., Liu, Q., Zhang, L., Calculation of the Added Mass of a Liquid Tank's Bulkheads, *Journal of Marine Science Application*, **13**, 41-48 (2014).

11 Inman, D. J., *Engineering Vibration*, 4th ed., Pearson Education Inc., 544-552 (2014).

12 Lamb, H., Hydrodynamics, 6th ed., Dover Publications, New York, pp. 66-85 (1945).

13 Newman, J. N., Marine Hydrodynamics, MIT Press, Cambridge, 145 (1977).

14 Kaneko, S., Nakamura, T., Inada, F., Kato, M., Ishihara, K., Nishihara, T., Mureithi, N. W., *Flow-Induced Vibrations*, 2nd ed. Elsevier Ltd., 361-365 (2014).

15 Holman, J. P., Heat Transfer, 4th ed., Chapter 1 (1976).